Spectrum of Engineering Sciences
ISSN (e) 3007-3138 (p) 3007-312X
Volume 3, Issue 10, 2025

STEADY STATE ELECTROMAGNETIC ANALYSIS OF THE SQUIRREL CAGE INDUCTION MOTOR

Qurban Ali Shah Syed[*1], Imtiaz Ali Laghari[2], Asif Ali[3], Kamran Ahmed Samo[4], Zuhebullah Soomro[5]

[*1, 2, 4, 5] *Department of Electrical Engineering, The University of Larkano, Pakistan*
[3] *Department of Mechanical Engineering, The University of Larkano, Pakistan*

[*1]qurban.syed@uolrk.edu.pk, [2]imtiaz.laghari@uolrk.edu.pk, [3]asifali@uolrk.edu.pk, [4]drkamranahmed@uolrk.edu.pk, [5]soomrozohaib17@gmail.com

DOI: https://doi.org/10.5281/zenodo.17481081

Keywords
asynchronous machine, finite element analysis, induction motor, slip analysis, squirrel cage rotor, steady state conditions.

Article History
Received: 11 September 2025
Accepted: 16 October 2025
Published: 30 October 2025

Corresponding Author: *
Qurban Ali Shah Syed

Abstract
This paper deals with the steady-state electromagnetic analysis of a squirrel cage induction motor (IM) and evaluates the squirrel cage IM's performance at different rotor positions, supplied voltages, rotor slips, and at different operating conditions of the no-load and the blocked-rotor cases. The squirrel cage IM's electromagnetic torque characteristic is analyzed to determine the base squirrel cage rotor's initial position relative to the stator, where the electromagnetic torque is constant over a cycle. The results are used to define the initial rotor position for further steady state analysis, ensuring accurate electromagnetic torque performance analysis at different rotor positions. The squirrel cage IM's performance at varying slip values is computed to explore its efficiency under different load conditions. Thus, the steady-state analysis computes key performance characteristics, including electromagnetic torque, current, losses and efficiency of the squirrel cage IM as a function of slip. The slip adjustment determines the operational efficiency and electromagnetic torque under rated load conditions and identifies the optimal slip value where the squirrel cage IM operates at maximum efficiency. A parametric study is carried out when the supplied voltage is varied at different operating conditions, and the study provides insights into the squirrel cage IM's performance during startup and under locked rotor conditions to develop accurate equivalent circuit models and optimizing the squirrel cage IM's design for various operational scenarios.

1. INTRODUCTION

Induction motors (IMs) are the base to industrial applications due to their robustness, reliability, and cost effectiveness, and are the most widely used electric motors, accounting for over 85% of applications involving rotating apparatus and consuming more than 60% of industrial electricity in developed countries [El-Shahat, A. et al., 2023], [Syed, Q.A.S. et al., 2025]. The squirrel cage type IMs are particularly favored for their simplicity, low maintenance, and high efficiency compared to the wound rotor type IMs [Lipo, T.A. 2017]. There are two main types of IMs, considering the rotor type, such as, a squirrel-cage IM and wound rotor IM. A squirrel cage IM is simple and rugged, whereas a wound-rotor IM provides better control over torque and speed [Boldea, I., et al. 2010].

A squirrel cage IM has two main parts, the stator and the rotor, as shown in Figure 1. The stator is stationary and consists of laminated electrical steel sheets to reduce the iron loss [Boldea, I., et al. 2010], [Kovács, K. 2022]. When a three-phase ac voltage supply is applied to the stator, it produces a rotating magnetic field. This rotating field cuts the stationary rotor bars of the squirrel cage IM, inducing electromotive force (EMF) due to Faraday's law of induction [Lipo, T.A. 2017]. The rotor of a squirrel cage IM always lags behind the rotating magnetic field; hence the term asynchronous motor is also used for the IM [Boldea, I., et al. 2010], [Bleizgys, V., et al. 2010]. A squirrel cage IM's rotor bars are short-circuited through end rings, flowing current induces their own magnetic field, and the interaction between the stator's rotatory field and the induced rotor field develops the desired electromagnetic torque, responsible for running the squirrel cage IM under load conditions.

Squirrel cage IMs have a robust design requiring less maintenance, and do not require brushes or commutators, which are common failure points [Boldea, I., et al. 2010]. Due to the reliability, cost-effectiveness, and ease of maintenance of the IMs, these are used across various sectors, including industrial, commercial, and domestic applications, such as pumps, fans, conveyors, household appliances, and even electric vehicles (EVs) [Azab, M. 2025], [Ahmed, S., et al. 2025]. Understanding the operation and torque-speed characteristics of these motors is a key to optimizing performance and efficiency, particularly in complex industrial environments.

Although, the steady-state electromagnetic behavior in IMs is analyzed by analytical, numerical or combination of both the methods, the finite element analysis (FEA) numerical method has been employed to determine the electromagnetic fields within the squirrel cage IM [Gherghina, I.-S., et al. 2025], [Wang, Y.-J., et al. 2011]. A steady-state electromagnetic analysis is foundation for the design, optimization, and performance evaluation of the squirrel cage IMs [Altair Engineering, Inc. 2025]. The 2D FEA provides key insights into parameters like electromagnetic torque, current, losses and efficiency, and is a simple numerical tool for designing squirrel cage IMs for optimal performance, reliability, and longevity. A steady state electromagnetic analysis focuses on understanding the motor's behavior under constant operating conditions, where transient effects have settled, and the system has reached stability [Xu, C., et al. 2019], [Xu, C., et al. 2017]. Thus, the squirrel cage IM operates at a constant speed, with stabilized current and electromagnetic fields [Di Nardo, M., et al. 2020].

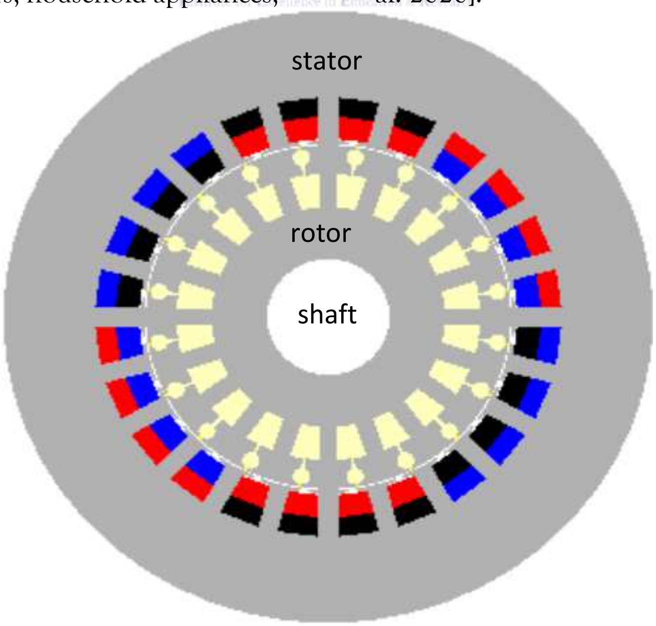

Figure 1: Three-phase squirrel cage IM.

2. SQUIRREL CAGE INDUCTION MOTOR

The squirrel cage IM has 2 poles, 24 stator slots for the stator coil winding and 20 rotor slots for the rotor bars. Stator winding is a double layer lap winding scheme, whereas, rotor of the IM is double squirrel cage, as shown in Figure 1. Rotor bars of the squirrel cage IM are of cast aluminum, and are interconnected by end rings, which help in the formation of the squirrel cage. This construction minimizes losses and enhances performance, especially under high-speed conditions. The stator winding uses copper conductors and is arranged in a two-layer configuration.

The geometrical design specifications of the squirrel cage IM are provided in Table 1. The outer diameter of the squirrel cage IM is 212 mm, while the average airgap diameter of the squirrel cage IM is 118.5 mm, and the shaft diameter is 40 mm. The axial length without the end winding length of the squirrel cage IM is 125 mm.

Table 1: Geometrical specifications of the squirrel cage IM.

Symbol	*Item*	*Value*
P	Rated load power	7.5 kW
V	Supply voltage	380 V
f	Frequency	50 Hz
S	Stator slots	24
R_{so}	Sator outer radius	106 mm
R_{ro}	Rotor outer radius	69.5 mm
R_s	Shaft radius	20 mm
g	Airgap	0.5 mm
L	Total axial length	125 mm
N	Number of windings turns per phase	208

3. METHODOLOGY

The FEA method is utilized to simulate the squirrel cage induction motor (IM), for analyzing the motor's output characteristics under various steady state operating conditions. The squirrel cage IM's geometry is defined using the Altair manual [Altair Engineering, Inc. 2025], then meshed into fine elements. The meshing must be fine, especially in areas like the rotor bars of the squirrel cage IM and the airgap where electromagnetic interactions are most significant. The airgap is divided into two parts, i.e., rotating airgap and stationary airgap, and fine meshing is done at the line dividing both the airgap regions.

The physical properties like specific materials are chosen from the material's manger and assigned to their respective regions of the squirrel cage IM, ensuring the material properties concerned. Mechanical parameters and physical application of steady state AC application are defined. To reduce the computation time of the 2D FEA, symmetry and periodicity of the squired cage IM is determined and the relevant boundary conditions are applied before solving the model. Electrical circuit is created and stator windings and their connections, rotor bars and their connections are assigned to the respective electrical circuit components.

The FEA software simulates the squirrel cage IM's response under various steady state conditions, such as different slip values, rotational speeds, and load conditions. The results of the simulation process include magnetic flux density, current, electromagnetic torque, losses and efficiency.

4. RESULTS AND DISCUSSIONS

4.1 Influence of the rotor position

The 2D FEA is carried out to determine the initial rotor position in relation to the stator for optimal electromagnetic torque production of the squirrel cage IM. The rotor position where the electromagnetic torque produced remained consistent over a cycle is identified, offering the average electromagnetic torque value. It is critical as it determines the most efficient alignment between the stator's rotating magnetic field and the rotor, which ultimately influences the squirrel cage IM's performance.

The rotor position varies from 0 to 18 degrees, and the corresponding electromagnetic torque values are computed and plotted in Figure 2. The results show that the electromagnetic torque has ripples, peaking at certain rotor positions and decreasing at others due to the interaction between the stator and rotor slots, thus, the electromagnetic torque values range from 7.69 Nm to 8.85 Nm, with the average electromagnetic torque of 8.16 Nm at a rotor position of 1.143°.

The electromagnetic torque ripples are due to the slot effects in both the rotor and stator of the squirrel cage IM, which create periodic fluctuations in the magnetic field. The optimal rotor position ensures that the squirrel cage IM operates with minimal fluctuation in electromagnetic torque, leading to a more stable and efficient performance, and the design of the squirrel cage IM is refined to minimize losses and improve its overall efficiency.

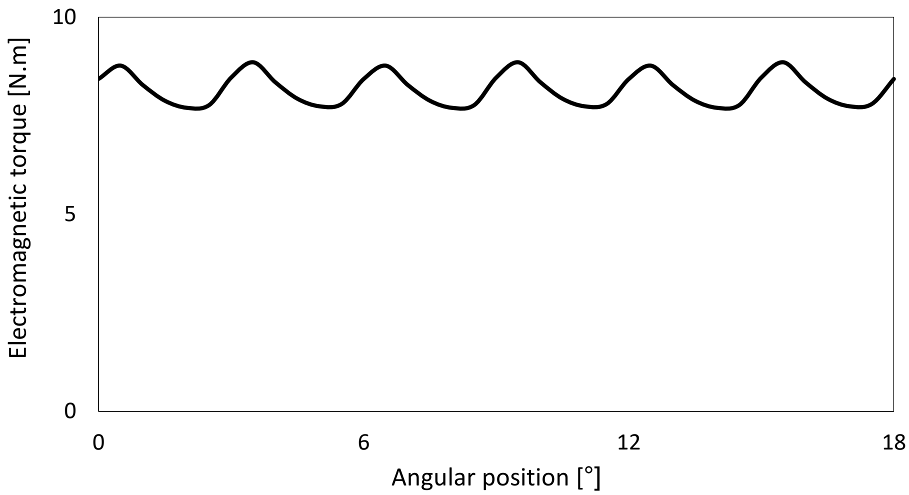

Figure 2: Electromagnetic torque of the squirrel cage IM at constant speed of 1% slip.

4.2 Influence of the rotor slip

The influence of the rotor slip at the rotor alignment of 1.143° on the squirrel cage IM's performance characteristics, including electromagnetic torque, current, losses, and efficiency is investigated using the 2D FEA. Rotor slip is the difference between the synchronous speed of the rotating magnetic field in the stator and the actual speed of the rotor, plays a critical role in determining the electromagnetic torque and overall efficiency of the squirrel cage IM. The current drawn by the squirrel cage IM is influenced by the rotor slip, thus when the slip varies the current characteristics change, as shown in Figure 3.

The influence of the rotor slip on the electromagnetic torque characteristics is shown in Figure 4. When the rotor slip increases, the electromagnetic torque output initially increases, peaking at an optimal slip value before starting to decrease. The maximum electromagnetic torque of 63.85 N.m for steady-state rated-load operation is achieved at a slip of 0.22. However, the rated slip value is determined to be 0.032, which corresponds to an output power equal to the motor's rated power.

The influence of the varying slip from 1% to 5% on the efficiency of the squirrel cage IM during steady state operation is shown in Figure 5. For a specific rated slip value of 0.032, the squirrel cage IM achieves an efficiency of 91.71 %, however, as the slip increases further, this efficiency sharply declines. Thus, determining the optimal slip for the rated output characteristics is crucial for squirrel cage IM's design and operation.

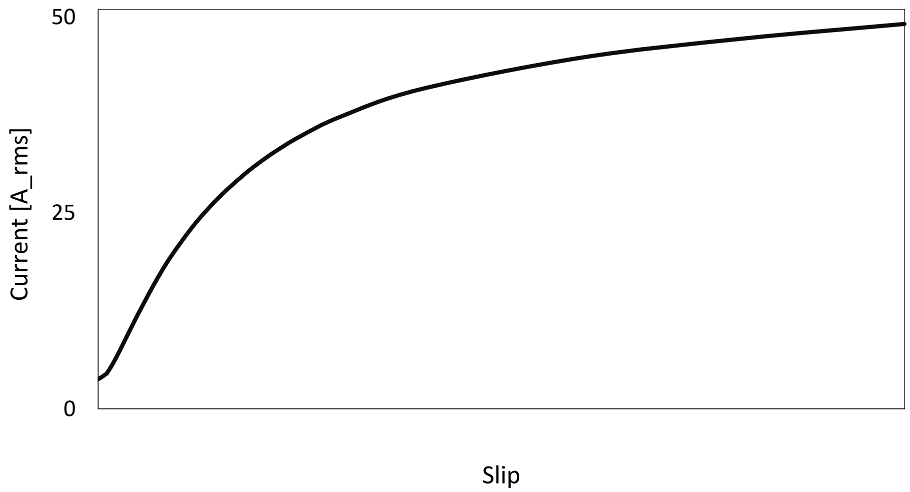

Figure 3: Influence of the slip on the drawn current of phase A by the squirrel cage IM.

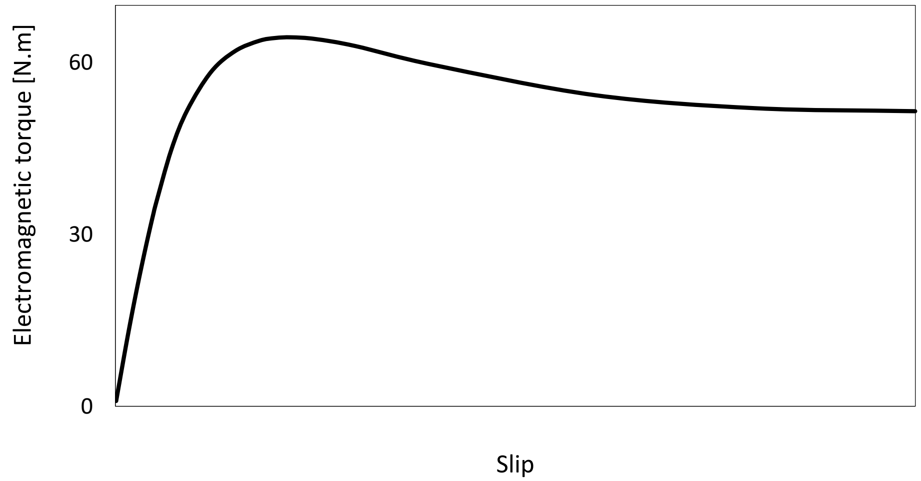

Figure 4: Influence of the slip on the electromagnetic torque of the squirrel cage IM.

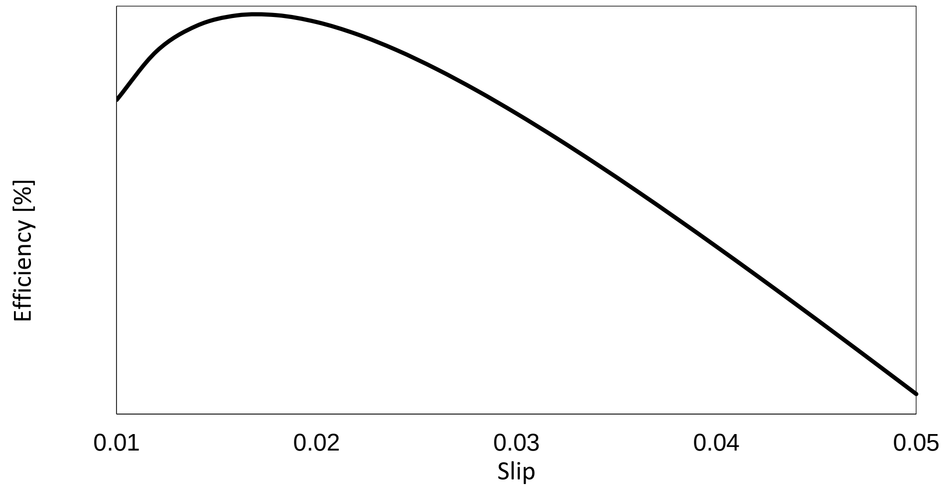

Figure 5: Influence of the slip on the efficiency of the squirrel cage IM.

4.3 Influence of the supplied voltage

A steady state computation using 2D FEA is performed to determine the equivalent circuit of the squirrel cage IM. The squirrel cage IM is supplied with a voltage of 15 ~ 30% of the nominal value to perform the locked-rotor test, whereas a no-load test is performed at a slip of 0.1% to analytically calculate the components of the equivalent circuit, such as rotor resistance and leakage inductance, and magnetization inductance and resistance for core losses.

The influence of the supplied voltage on the current drawn by the squirrel cage induction motor is shown in Figure 6. As the supply voltage increases from 60 V to 120 V, the current also increases proportionally. Thus, for a nominal required current of 8.48 A, the corresponding voltage supply is 94.478 V. Similarly, the active power of the squirrel cage IM is significantly influenced by the supplied voltage, as depicted in Figure 7. Thus, when the voltage supply increases, the active power also increases.

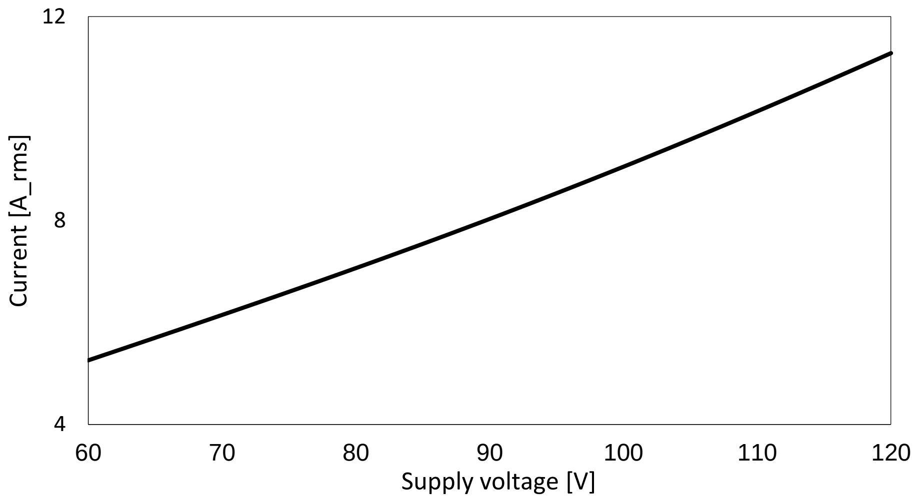

Figure 6: Influence of the supplied voltage on the drawn current of the squirrel cage IM.

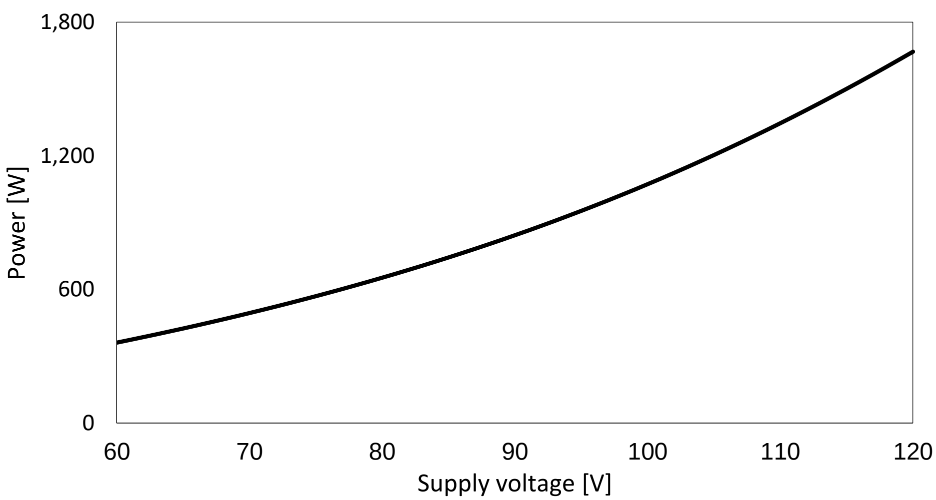

Figure 7: Influence of the supplied voltage on the active power of the squirrel cage IM.

The supplied voltage significantly influences the Joule losses in the stator core of the squirrel cage IM. As the voltage supply increases, the Joule losses in the stator core also increases, as shown in Figure 8, therefore, the supplied voltage directly impacts the thermal performance and efficiency of the motor due to increased resistive heating in the stator windings. At the supplied voltage of 94.478 V, the corresponding losses are 332.77 W. The no-load characteristics of the squirrel cage IM are determined by analyzing its behavior under no-load conditions, and the magnetic flux density across the squirrel cage IM is displayed in Figure 9 (a), whereas, under locked-rotor conditions the magnetic flux density across the squirrel cage IM is displayed in Figure 9 (b). The dark blue color represents the low flux density of 0 T, whereas light blue color represents the higher flux density of 2.15 T.

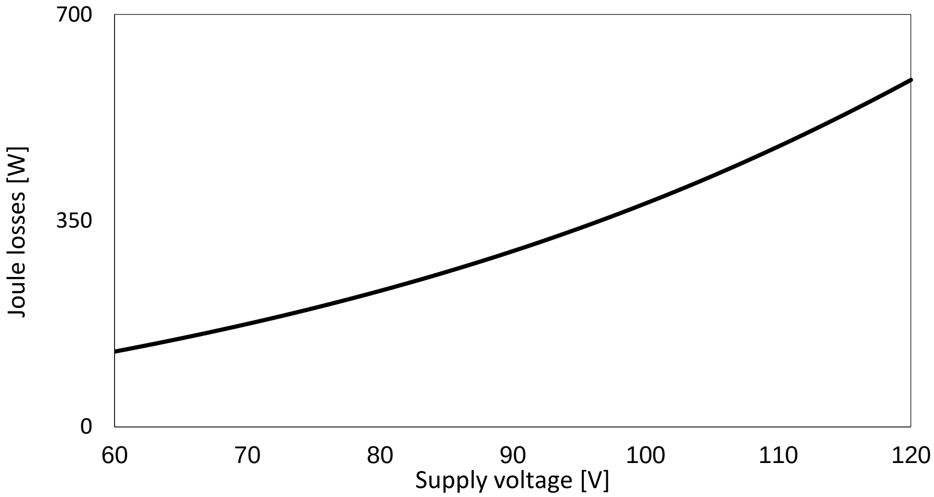

Figure 8: Influence of the supplied voltage on the power losses of the squirrel cage IM.

(a) (b)

Figure 9: Magnetic flux density of the squirrel cage IM under different operational conditions: (a) at no-load condition, and (b) at locked-rotor condition.

5. CONCLUSION:

The steady-state electromagnetic behavior of the squirrel cage IM is examined using the 2D FEA. The results offer critical insights into squirrel cage IM's performance under various operational conditions of different values of rotor position, slip, and voltage. The rotor position where the electromagnetic torque is consistent is determined for the enhanced motor efficiency. The influence of rotor slip on electromagnetic torque and efficiency is analyzed, and an optimal slip for the maximum performance of the squirrel cage IM is computed. The parametric analysis of varying the supply voltage affecting the squirrel cage IM's current, active power, and losses is carried out. This investigation is utilized to determine the equivalent circuit components of the squirrel cage IM. The steady-state analysis contributes to studying the squirrel cage IM's behavior during startup and under locked rotor conditions, which is important for motor protection and optimization.

Acknowledgement
Corresponding author acknowledges the support of Altair® for the 3D FEA license during the PhD research at the chair of Electrical Drives and Machines, FAU University of Erlangen-Nuremberg. The simulation and technical process is adopted from the Flux 2D solver manual.

References:

[1] Syed, Q.A.S., Shah, M.A., Ali, M., & Soomro, Z. (2025). Transient analysis of the squirrel cage induction. *Spectrum of Engineering Sciences*. In parallel publication process.

[2] El-Shahat, A., Ali, D., Thirugnanam, P., Tran, T., Brandštetter, P., Kuchař, M., Omar, F., Islam, A. S., Adib, A., Dhaouadi, R., Habibullah, T., Debanath, H., Sabbir, A. K. M., Belbali, S., Makhloufi, A., Kadri, L., Abdallah, Z., Seddik, Y., Zorgani, S., Hajji, Y., Koubàa, M., Boussak, S., Toumi, M., Benbouzid, M., Mimouni, S., Dabour, M., Hussien, A. M., Aboushady, M., Sen, K. K., Tran, T. C., Islam, A., Islam, A., Habibullah, M., Debanath, T., & Sabbir, M. S. H. (2023). *Induction motors - Recent advances, new perspectives and applications*. IntechOpen. https://doi.org/10.5772/intechopen.104031

[3] Lipo, T.A. (2017). *Introduction to AC machine design*. Wiley. https://doi.org/10.1002/9781119352181

[4] Boldea, I., & Nasar, S. A. (2010). *The induction machine handbook*. CRC Press, Taylor & Francis Group.

[5] Kovács, K. (2022, September 5). Influence of the rotor slot numbers on the parasitic torques and the radial magnetic forces of the squirrel cage induction motor: An analytic approach. *International Conference on Electrical Machines*, Valencia, Spain. https://doi.org/10.1109/ICEM51905.2022.9910

[6] Bleizgys, V., & Baskys, A. (2010). The influence of supply voltage amplitude variation law on AC induction motor efficiency in variable-speed drive. *Solid State Phenomena, 164*, 1–6. https://doi.org/10.4028/www.scientific.net/SSP.164.1

[7] Azab, M. (2025). A review of recent trends in high-efficiency induction motor drives. *Vehicles, 7*(1), 15. https://doi.org/10.3390/vehicles7010015

[8] Ahmed, S., Aarniovuori, L., Nerg, J., Barta, J., & Vitek, O. (2025). Emerging trends in high-speed induction machines and converter technologies for industrial applications. In *2025 IEEE International Electric Machines & Drives Conference (IEMDC)* (pp. 409-414). IEEE. https://doi.org/10.1109/IEMDC60492.2025.11061054

[9] Gherghina, I.-S., Bizon, N., Iana, G., & Vasilică, B.-V. (2025). Recent advances in fault detection and analysis of synchronous motors: A review. *Machines, 13*(9), 815. https://doi.org/10.3390/machines13090815

[10] Wang, Y.-J., Lee, M.-H., & Sung, S.-W. (2011, September). Analytical modeling of pulsating torques of induction motors caused by supply voltage unbalance. Paper presented at the *International Conference on Universal Energy and Environmental Protection (ICUEPES)*, Taipei, Taiwan. IEEE.

[11] Altair Engineering, Inc. (2025). *Altair Flux 2D* [Finite element software for low-frequency electromagnetic and thermal simulations]. https://altair.com/flux

[12] Xu, C., Zhang, Z., Yu, L., & Bian, Z. (2019, August). Influence of rotor position error on the torque performance of doubly salient electromagnetic motor drives. Paper presented at the *International Conference on Electrical Machines and Systems (ICEMS)*, Harbin, China. IEEE.

[13] Xu, W., Bao, X., Di, C., Wang, L., & Chen, Y. (2017). Optimal angle combination for improving electromagnetic torque in induction motor with double-skewed rotor. *IEEE Transactions on Magnetics, 53*(11), 1–4. https://doi.org/10.1109/TMAG.2017.2739602

[14] Di Nardo, M., Marfoli, A., Degano, M., Gerada C., & Chen, W. (2020). Rotor design of squirrel cage induction motor - part II: Results discussion. *IEEE*, 1–9. https://doi.org/10.1109/TIE.2019.2922094